(Table IV) indicating that the azido group is nonlinearly coordinated to Cu(II).[24]

There is a broad absorption in the range 3200-3600 cm^{-1} associated with the N-H stretch and coordinated/lattice water.

IR data support the stoichiometry/structure proposed for the above complexes (Figure 9).

Acknowledgment. G.B. acknowledges a JRF award from the University Grants Commission, New Delhi, India. We are also thankful to Dr. V. K. Singh for assisting in the EPR work.

(24) Forster, D.; Horrocks, W. D. *Inorg. Chem.* **1966**, *5*, 1510-1514.

Contribution from the Department of Chemistry, School of Science and Engineering, Waseda University, Shinjuku-ku, Tokyo 169, Japan

Surface-Enhanced Resonance Raman Scattering Study on the Axial Ligation States of Manganese and Chromium Tetraphenylporphines Adsorbed on Silver Electrode Surfaces

Tatsushi Okumura, Shigeru Endo, Akio Ui, and Koichi Itoh*

Received June 25, 1991

Surface-enhanced resonance Raman scattering spectra (SERRS) in the region below 500 cm^{-1} were recorded for the manganese(III) and chromium(III) tetraphenylporphine complexes (TPP)$Mn^{III}X$ (X = Cl^-, ClO_4^-) and (TPP)$Cr^{III}X$ (X = Cl^-, ClO_4^-) adsorbed on a silver electrode surface in acetonitrile (ACN). The surface spectra in the low-frequency region clearly reflect changes in the axial ligation states of the metalloporphines associated with the adsorption process involving the silver electrode. On adsorption to the electrode at 0 V (vs Ag/AgCl), (TPP)$Mn^{III}Cl$ dissociates the fifth axial ligand (a chloride ion), forming an adsorbed species, $[(TPP)Mn^{III}]^+$. On the other hand, (TPP)$Cr^{III}Cl$ retains the chloride ion as a fifth axial ligand on the electrode surface at 0 V. Upon a negative sweep of the electrode potential, the chloride complex gradually disappears, forming $[(TPP)Cr^{III}]^+$; the disappearance is completed at -0.4 V. A SERRS spectrum obtained for a divalent manganese TPP complex adsorbed on a silver electrode proved that the adsorbate is a four-coordinated species; in contrast, the divalent manganese complex in ACN exists as a five-coordinated complex possessing an associated solvent molecule as a fifth ligand (i.e., (TPP)Mn^{II}(ACN)).

Introduction

Surface-enhanced resonance Raman scattering (SERRS) spectroscopy has been recognized as one of the most sensitive techniques to observe the vibrational spectra of various chromophores,[1-3] including heme proteins[4-8] and chlorophylls[9,10] adsorbed on coinage metals such as silver and gold. Its high sensitivity permits acquisition of the vibrational spectra of adsorbates even at a surface coverage less than a monomolecular layer. Surface spectra have been measured also for synthetic metalloporphines adsorbed on silver electrodes,[11-14] silver colloids,[15] and roughened silver surfaces;[16] the results revealed characteristic features of their surface processes including redox reactions and metal-insertion and -exchange reactions.

In the present paper, we report the SERRS spectra of adsorbates on a silver electrode for manganese(III) and chromium(III) tetraphenylporphines having an axially coordinated monoanion, such as chloride and perchlorate, in acetonitrile (ACN); the manganese and chromium complexes are abbreviated as (TPP)$Mn^{III}X$ (X = Cl^-, ClO_4^-) and (TPP)$Cr^{III}X$ (X = Cl^-, ClO_4^-), respectively. The SERRS spectra were also recorded for (TPP)Mn^{II} and (TPP)Cr^{II}, which were electrochemically generated on the surface from the corresponding trivalent complexes. During the analysis of the surface spectra, we confined our attention to the elucidation of changes in the ligation states of the metalloporphines caused by adsorption to the silver electrode surface. With regard to the ligation states in solutions, electrochemical, spectrophotometric, and conductometric studies have been performed on the manganese[17] and chromium[18-20] complexes, revealing the following points. (i) (TPP)$Mn^{III}ClO_4$ and (TPP)-$Cr^{III}ClO_4$ dissociate the perchlorate ion in ACN, forming $[(TPP)Mn^{III}]^+$ and $[(TPP)Cr^{III}]^+$, respectively. (ACN may associate with the manganese and chromic complexes, forming $[(TPP)Mn^{III}(ACN)_2]^+$ and $[(TPP)Cr^{III}(ACN)_2]^+$, respectively. Actually, this type of six-coordination state has been postulated for the trivalent complexes in dimethylformamide and pyridine, which are more strongly coordinating solvents than ACN.[17,19] In this paper, however, the coordination of ACN to the trivalent complexes is neglected because we have not obtained direct evidence for the coordination.) (ii) (TPP)$Mn^{III}Cl$ and (TPP)$Cr^{III}Cl$ in ACN retain the chloride ion as a fifth axial ligand. On the other hand, no direct measurement has been performed to clarify the ligation states of the manganese and chromium complexes adsorbed on electrode surfaces. A clarification of the ligation states of the metalloporphines adsorbed on the electrode surfaces is of crucial importance to the analysis of their electrochemical properties, because an electron transfer should take place between the adsorbates and the electrode surfaces during the redox reactions of the complexes. From comparison of the SERRS and RRS spectra of the trivalent and divalent complexes, we found that the SERRS features in the low-frequency region (below 500 cm^{-1})

(1) Van Duyne, R. P. In *Chemical* and *Biological Application of Lasers*; Moore, C. B., Ed.; Academic Press: New York, 1979; Vol. 4, Chapter 5.
(2) Moskovits, M. *Rev. Mod. Phys.* **1985**, *57*, 783.
(3) Cotton, T. M. In *Spectroscopy of Surfaces*; Clark, R. J., Hester, R. E., Eds.; John Wiley & Sons: Chichester, U.K., 1988; Chapter 3.
(4) Cotton, T. M.; Schultz, S. G.; Van Duyne, R. P. *J. Am. Chem. Soc.* **1980**, *102*, 7960.
(5) Copeland, R. A.; Foder, S. P. A.; Spiro, T. G. *J. Am. Chem. Soc.* **1984**, *106*, 3872.
(6) Smulvevich, G.; Spiro, T. G. *J. Phys. Chem.* **1985**, *89*, 5168.
(7) Hildebrandt, P.; Stockburger, M. *J. Phys. Chem.* **1986**, *90*, 6017.
(8) de Groot, J.; Hester, R. E.; Kaminaka, S.; Kitagawa, T. *J. Phys. Chem.* **1988**, *92*, 2044.
(9) Cotton, T. M.; Van Duyne, R. P. *FEBS Lett.* **1982**, *147*, 81.
(10) Hildebrandt, P.; Spiro, T. G. *J. Phys. Chem.* **1988**, *92*, 3355.
(11) Cotton, T. M.; Schultz, S. G.; Van Duyne, R. P. *J. Am. Chem. Soc.* **1982**, *104*, 6528.
(12) Itabashi, N.; Kato, K.; Itoh, K. *Chem. Phys. Lett.* **1983**, *97*, 528.
(13) Koyama, T.; Yamaga, M.; Kim, M.; Itoh, K. *Inorg. Chem.* **1985**, *24*, 4258.
(14) Sanchez, L. A.; Spiro, T. G. *J. Phys. Chem.* **1985**, *89*, 753.
(15) Itoh, K.; Sugii, T.; Kim, M. *J. Phys. Chem.* **1988**, *92*, 1568.
(16) Kobayashi, Y.; Itoh, K. *J. Phys. Chem.* **1985**, *89*, 5174.
(17) Kelly, S. L.; Kadish, K. M. *Inorg. Chem.* **1982**, *21*, 3631.
(18) Summerville, D. A.; Jones, R. D.; Hoffman, B. M.; Basolo, F. *J. Am. Chem. Soc.* **1977**, *99*, 8195.
(19) Bottomley, L. A.; Kadish, K. M. *Inorg. Chem.* **1983**, *22*, 342.
(20) Kelley, S. L.; Kadish, K. M. *Inorg. Chem.* **1984**, *23*, 679.

0020-1669/92/1331-1580$03.00/0

clearly reflect the ligation states of the manganese and chromium complexes adsorbed on the silver electrode surface. The present study is the first successful attempt to observe directly the coordination states of the manganese and chromium TPP complexes on the surface.

Experimental Section

Materials. (TPP)$Mn^{III}Cl$ was synthesized by the method of Adler et al.,[21] and (TPP)$Mn^{III}ClO_4$, by the method of Landrum et al.[22] (TPP)$Cr^{III}Cl$ was obtained through the method of Summerville et al.[18] Synthesis of (TPP)$Cr^{III}ClO_4$ was carried out by following the procedure of Kelly and Kadish.[17] (TPP)Mn^{II} and (TPP)Mn^{II}(4-Mepip) (4-Mepip = 4-methylpiperazine) in toluene solutions were prepared by the method of Gonzalez et al.[23] Briefly, (TPP)Mn^{II} was prepared by sodium borohydride reduction of (TPP)$Mn^{III}Cl$ in a CH_3OH–CH_2Cl_2 mixed-solvent system, dried under vacuum, and dissolved in toluene. All the procedures were performed using a vacuum line and Schlenk glassware because the divalent complex is very sensitive to air. (TPP)Mn^{II}(4-Mepip) was prepared by adding 1 equiv of 4-Mepip to a toluene solution of the complex. ACN was purified by distillation after treatment with calcium hydride. Toluene was treated with 4A molecular sieve and distilled under vacuum prior to use. Tetrabutylammonium perchlorate (TBAP) was purified by recrystallization three times from ethyl acetate.

Measurements. SERRS and RRS spectra were acquired with a JEOL Model 400D spectrometer equipped with a photon-counting system (Hamamatsu Photonics Type HTV-R943-02). An Ar^+ laser (NEC Model 3300GL) was used as the excitation source.

The electrochemical cell used for the SERRS measurements has been described previously.[12,13] A Ag/AgCl electrode (saturated KCl solution) was used as the reference electrode. The anodization of the silver working electrode was accomplished as follows: The electrode potential of an electrochemical cell containing 0.025 mol/L TBAP in ACN was swept from −0.5 to +0.5 V, kept at +0.5 V until a total oxidation current of 100 mC was passed through the electrode, and then stepped back to −0.5 V. After the anodization, each sample solution in ACN was added to the cell at 0 V up to a concentration level of about 1×10^{-4} mol/L. The thickness between the cell window and the electrode surface was made as small as possible to prevent interference of RRS scattering from the bulk solution. The 476.5-nm Ar^+ laser line was used for the acquisition of the SERRS spectra of the trivalent manganese complex, and the 457.9-nm line, for the acquisition of the SERRS spectra of the divalent manganese complex as well as the SERRS spectra of the trivalent and divalent chromium complexes.

A Raman spectroelectrochemical cell[13] was used for the acquisition of the RRS spectra of (TPP)$Mn^{III}Cl$, (TPP)$Mn^{III}ClO_4$, (TPP)$Cr^{III}Cl$, and (TPP)$Cr^{III}ClO_4$ in ACN and for the acquisition of the RRS spectra of the corresponding divalent complexes; controlled-potential electrolysis was performed at −0.5 V for the preparation of (TPP)Mn^{II} and at −1.0 V for (TPP)Cr^{II}. The RRS spectra of (TPP)Mn^{II} and (TPP)Mn^{II}(4-Mepip) in toluene were recorded by using a Pyrex cell attached to a Schlenk tube without exposing the solutions to air. The 476.5-nm Ar^+ laser line was used to excite the RRS spectra of the manganese(III) complexes, and the 457.9-nm line was used to excite the RRS spectra of the manganese(II) and the chromium(III/II) complexes.

Results and Discussion

RRS and SERRS Spectra of (TPP)$Mn^{III}X$ ($X = Cl^-, ClO_4^-$) in ACN. Parts A and C of Figure 1 present the RRS spectra, in the frequency region below 600 cm^{-1}, observed for (TPP)$Mn^{III}Cl$ and (TPP)$Mn^{III}ClO_4$ in ACN. The RRS spectra in the 1600–800-cm^{-1} region (not shown) of both complexes exhibit the characteristic features[24] of trivalent manganese TPP complexes, giving rise to ν_2 ($\nu(C_\beta$–$C_\beta)$, A_{1g}) at 1560 cm^{-1} and ν_4 ($\nu(C_\alpha$–N), A_{1g}) at 1375 cm^{-1}. On the other hand, the RRS spectrum in the low-frequency region observed for (TPP)$Mn^{III}Cl$ is quite different from that of (TPP)$Mn^{III}ClO_4$ in ACN; i.e., the RRS bands at 295 and 246 cm^{-1} observed for the former complex are absent in the RRS spectrum of the latter. Recently, Spiro and co-workers[25,26] made extensive assignments of the RRS and infrared

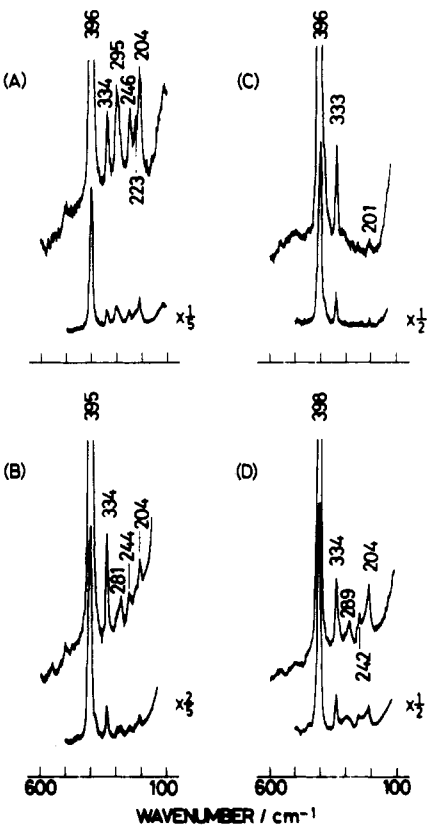

Figure 1. Comparison of the RRS and SERRS spectra of (TPP)$Mn^{III}X$ ($X = Cl^-, ClO_4^-$) in ACN: (A) RRS spectrum of (TPP)$Mn^{III}Cl$, concentration of sample solution (c) = 2.5×10^{-4} mol/L; (B) SERRS spectrum measured at 0 V for (TPP)$Mn^{III}Cl$, $c = 5.1 \times 10^{-5}$ mol/L; (C) RRS spectrum of (TPP)$Mn^{III}ClO_4$, $c = 2.6 \times 10^{-4}$ mol/L; (D) SERRS spectrum measured at 0 V for (TPP)$Mn^{III}ClO_4$, $c = 5.7 \times 10^{-5}$ mol/L. Excitation wavelength = 476.5 nm. Laser power = 180 (A), 100 (B), 120 (C), and 60 mW (D). Spectral slit width = 7 cm^{-1}.

spectra of (TPP)Ni^{II} with the aid of normal-coordinate calculations. According to their results, the 396-cm^{-1} band in Figure 1A is the counterpart of the 402-cm^{-1} band (ν_8 (A_{1g})) of (TPP)Ni^{II} and is ascribable mainly to a Ni–N stretching vibration. The 334- and 246-cm^{-1} bands correspond to the 330- and 251-cm^{-1} bands of (TPP)Ni^{II}, which are assigned to out-of-plane porphine ring vibrations, γ_2 (A_{1u}, a pyrrole swivelling vibration) and γ_7 (A_{2u}, a C_α–C_m bending vibration), respectively. The RRS band at 204 cm^{-1} in Figure 1A corresponds to the 202-cm^{-1} band of (TPP)Ni^{II}, which is assigned to ϕ_{10} (A_{1g}), associated with the in-phase stretching mode of the four C_m–Ph bonds. (In this mode, all the phenyl groups move in the same direction as the C_m–Ph bonds stretch.) It is not clear whether the 295-cm^{-1} band in Figure 1A is assigned to ν_{18} (B_{1g}), mainly due to a metal–N stretching vibration, or to an out-of-plane porphine ring vibration, γ_6 (A_{2u}, a pyrrole tilting vibration). In ACN, the (TPP)$Mn^{III}X$ complexes, where $X = SCN^-$, Br^-, and I^-, give rise to RRS bands at 284, 278, and 273 cm^{-1}, respectively;[27] these bands correspond to the 295-cm^{-1} RRS band observed for (TPP)$Mn^{III}Cl$. All the ligands are known to coordinate to the central manganese(III) ion, as in the case of the chloride ion of (TPP)$Mn^{III}Cl$ in ACN.[17] Then, the frequency dependence of the RRS bands on the kind of ligands suggests that the vibrational mode of the 295-cm^{-1} band also contains out-of-plane components which can couple with a Mn–Cl stretching vibration. The infrared spectrum of (TPP)$Mn^{III}Cl$ in a KBr disk gives rise to prominent peaks at 295 and 287 cm^{-1},[27] either one of which may be the counterpart of the 295-cm^{-1} RRS

(21) Adler, A. D.; Longo, F. R.; Kampas, F.; Kim, J. *J. Inorg. Nucl. Chem.* **1970**, *32*, 2443.
(22) Landrum, J. T.; Hatano, K.; Scheidt, W. R.; Reed, C. A. *J. Am. Chem. Soc.* **1980**, *102*, 6729.
(23) Gonzalez, B.; Kouba, J.; Yee, S.; Reed, C. A. *J. Am. Chem. Soc.* **1975**, *97*, 3247.
(24) Parthasarathi, N.; Hansen, C.; Yamaguchi, S.; Spiro, T. G. *J. Am. Chem. Soc.* **1987**, *109*, 3865.
(25) Li, X.-Y.; Czernuszewicz, R. S.; Kincaid, J. R.; Su, Y. O.; Spiro, T. G. *J. Phys. Chem.* **1990**, *94*, 31.
(26) Li, X.-Y.; Czernuszewicz, R. S.; Kincaid, J. R.; Spiro, T. G. *J. Am. Chem. Soc.* **1989**, *111*, 7012.
(27) Endo, S.; Okumura, T.; Itho, K. Unpublished work.

band. These results are in favor of the assignment to γ_6.

As Spiro and co-workers pointed out,[26] the appearance of the out-of-plane porphine ring vibrations of A_{1u} and A_{2u} symmetries is mainly due to a lowering of the porphine ring symmetry from D_{4h}; the lowering causes intensity borrowing of the out-of-plane modes from in-plane modes through vibrational mixing; the in-plane vibrations can be resonance enhanced via $\pi-\pi^*$ transitions (B and Q bands). The Mn–Cl stretching mode may also mediate a vibrational mixing between in-plane and out-of-plane vibrations, causing intensity borrowing of the out-of-plane vibrations from in-plane porphine ring vibrations. As already explained, (TPP)$Mn^{III}ClO_4$ dissociates the perchlorate ion in ACN.[17] It is reasonable to consider that the dissociated complex assumes a less deformed structure compared to an associated complex such as (TPP)$Mn^{III}Cl$. Presumably, such a structural change in the porphine ring and the absence of the Mn–Cl stretching mode cause the decrease in the intensity-borrowing effect of the dissociated complex, resulting in the disappearance of the 295- and 246-cm^{-1} bands in Figure 1C.

Parts B and C of Figure 1 show the SERRS spectra of (TPP)$Mn^{III}Cl$ and (TPP)$Mn^{III}ClO_4$, respectively, adsorbed on a silver electrode in ACN (at 0 V). Comparison of the SERRS spectrum of (TPP)$Mn^{III}Cl$ to that of (TPP)$Mn^{III}ClO_4$ indicates that the features of the surface spectra are similar, suggesting that the structures of the adsorbates from (TPP)$Mn^{III}Cl$ and $[(TPP)Mn^{III}]^+$ in ACN on the silver electrode surface are almost identical. (As already mentioned, (TPP)$Mn^{III}ClO_4$ in ACN assumes a dissociated state, i.e., $[(TPP)Mn^{III}]^+$.[17]) Thus, on adsorption to the electrode surface, (TPP)$Mn^{III}Cl$ releases the axial chloride ligand and exists as $[(TPP)Mn^{III}]^+$ at the electrode. The surface spectra of the adsorbates from (TPP)$Mn^{III}Cl$ and $[(TPP)Mn^{III}]^+$ in ACN (Figure 1B,D) exhibit bands near 285 and 243 cm^{-1}, which are absent in the RRS spectrum of $[(TPP)Mn^{III}]^+$ in ACN (Figure 1C). The 285- and 243-cm^{-1} bands correspond to the 295- and 246-cm^{-1} bands in Figure 1A and are ascribable to γ_6 (A_{2u}) and γ_7 (A_{2u}), respectively. The adsorption process may cause the porphine ring of $[(TPP)Mn^{III}]^+$ to assume a more deformed structure compared to that in the solution, resulting in the appearance of out-of-plane vibrations due to the above-mentioned intensity-borrowing effect.

RRS and SERRS Spectra of (TPP)Mn^{II}. Parts A and B of Figure 2 show the RRS spectrum of (TPP)Mn^{II} in ACN and the SERRS spectrum recorded at −1.0 V for the divalent complex adsorbed on a silver electrode, respectively. The band at 258 cm^{-1} in the RRS spectrum is absent in the SERRS spectrum. In order to assign the 258-cm^{-1} band, we recorded the RRS spectra of (TPP)Mn^{II}(4-Mepip) (4-Mepip = 4-methylpiperazine) and (TPP)Mn^{II} in toluene, which are shown in Figure 2, parts C and D, respectively; the former complex is five-coordinated (having 4-Mepip attached to the central metal ion) and the latter is four-coordinated.[23] From the spectra we can conclude that the 250-cm^{-1} band in Figure 2C is characteristic of the five-coordinated complex. A corresponding band is observed at 263 cm^{-1} for (TPP)Mn^{II} in dimethylformamide (DMF), consistent with its formulation as (TPP)Mn^{II}(DMF).[27] The 258-cm^{-1} band in Figure 2A is the counterpart of the 250-cm^{-1} band observed for (TPP)Mn^{II}(4-Mepip) and the 263-cm^{-1} band for (TPP)Mn^{II}-(DMF). (TPP)Mn^{II} in ACN is also in a five-coordinated state; ACN is probably coordinated to the manganese(III) ion through the nitrogen atom. The absence of the band corresponding to the 258-cm^{-1} band in the surface spectrum of Figure 2B indicates that the divalent absorbate assumes a four-coordination state, as in the case of (TPP)Mn^{II} in toluene.

The RRS and SERRS spectra of (TPP)Mn^{II} (Figure 2A,B) each show a band at 377 cm^{-1}, which is shifted from the band near 395 cm^{-1}, assigned to the ν_8 (A_{1g}) mode of the trivalent complex[26] (Figure 1A,B). The frequency shift may be attributed mainly to a structural change caused by the reduction of the central metal of the manganese complexes from the trivalent to the divalent state.

RRS and SERRS Spectra of (TPP)$Cr^{III}X$ (X = Cl^-, ClO_4^-) and (TPP)Cr^{II}. Figure 3 summarizes the electrode-potential dependence of the RRS spectra of (TPP)$Cr^{III}Cl$. A cathodic peak for the reduction of (TPP)$Cr^{III}Cl$ to the divalent state has been observed at −1.00 V (vs SCE) in propionitrile and at −0.88 V in DMF.[19] The spectra recorded at 0 and −0.5 V (Figure 3A,B) exhibit almost identical features, which indicates that the complex in ACN assumes an almost identical structure, keeping a trivalent state at these potentials. The spectrum in Figure 3C, which was observed after completion of controlled-potential electrolysis at −1.0 V, is quite different from that of the trivalent complex. The band at 399 cm^{-1} due to the ν_8 mode shifts to 389 cm^{-1} for the divalent complex. In addition, the overall intensities of the RRS bands are definitely reduced on conversion from the trivalent to the divalent state. The spectra in Figure 3 were obtained with 457.9-nm excitation, and at least a part of the intensity decrease is attributed to the reduction in the resonance enhancement effect associated with the shift of the Soret band from 443 nm (observed for the trivalent complex in ACN) to 435 nm (the divalent complex).

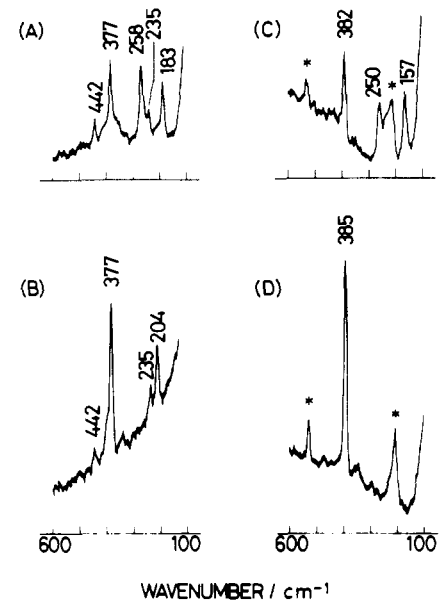

Figure 2. Comparison between the RRS spectra (A, C, D) of (TPP)Mn^{II} in various ligation states and the SERRS spectrum (B) measured at −1.0 V for (TPP)Mn^{II} in ACN: (A) RRS spectrum of (TPP)Mn^{II} in ACN, concentration of the sample (c) = 3.9×10^{-4} mol/L; (B) SERRS spectrum measured at −1.0 V for (TPP)Mn^{II}, c = 5.1×10^{-5} mol/L; (C) RRS spectrum of (TPP)Mn^{II}(4-Mepip) in toluene, c = ca. 4×10^{-4} mol/L; (D) RRS spectrum of (TPP)Mn^{II} in toluene, c = ca. 5×10^{-4} mol/L. The asterisks in spectra C and D are due to the solvent. Excitation wavelength = 457.9 nm. Laser power = 100 (A), 20 (B), 80 (C), 90 mW (D). Spectral slit width = 8 cm^{-1}.

Parts D–F of Figure 3 illustrate the electrode potential dependence of the SERRS spectra of (TPP)$Cr^{III}Cl$. The surface spectrum measured at 0 V is almost identical with the RRS spectra in Figure 3A,B, except for a weak feature near 277 cm^{-1} observed in the latter spectra. As shown in Figure 3D,E, upon a sweep of the electrode potential from 0 to −0.3 V, the surface spectra exhibit an appreciable decrease in the intensity ratio of the 358-cm^{-1} band to the 400-cm^{-1} band. As mentioned below, a cyclic voltammogram observed for (TPP)$Cr^{III}Cl$ in ACN using an anodized silver electrode gives rise to a reduction peak at −0.79 V. Then, in the potential region from 0 to −0.3 V the adsorbate retains its trivalent state. When the electrode potential is stepped further to −1.0 V, the intensity of the bands observed for the surface spectra is appreciably reduced, giving the surface spectrum in Figure 3F. The intensity decrease, which, as mentioned above, was observed also for the RRS spectra (Figure 3B,C), suggests that the potential step to −1.0 V causes the reduction of the adsorbate from the trivalent to the divalent state. The ν_8 mode of the adsorbate at −1.0 V, however, was observed at 400 cm^{-1}, which is appreciably higher than the corresponding band observed for the RRS spectrum of the divalent complex at −1.0 V (Figure 3C). Plausibly, the adsorption process fixes the porphine ring structure of the

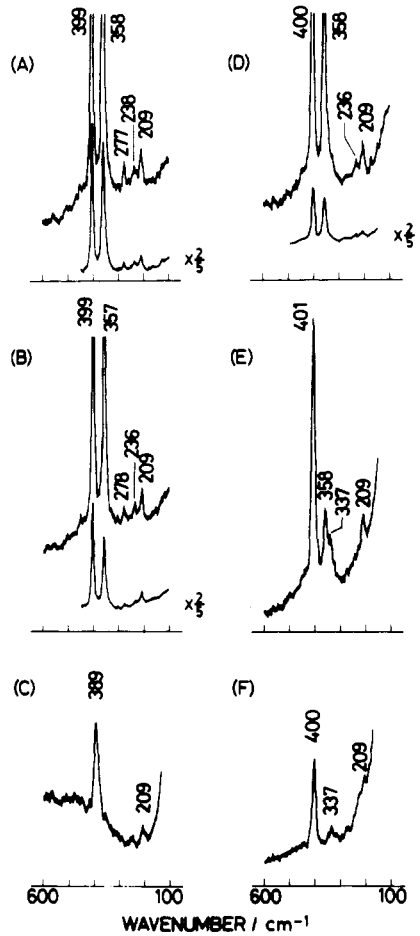

Figure 3. Electrode potential dependence of the RRS spectra (A–C) and the SERRS spectra (D–F) of (TPP)$Cr^{III}Cl$ in ACN (concentration of sample solution for RRS measurement 2.3×10^{-4} mol/L; concentration for SERRS measurement 8.0×10^{-5} mol/L): (A) at 0 V; (B) at −0.5 V; (C) at −1.0 V; (D) at 0 V; (E) at −0.3 V; (F) at −1.0 V. Excitation wavelength = 457.9 nm. Laser power = 90 (A–C) and 30 mW (D–F). Spectral slit width = 7 cm^{-1}.

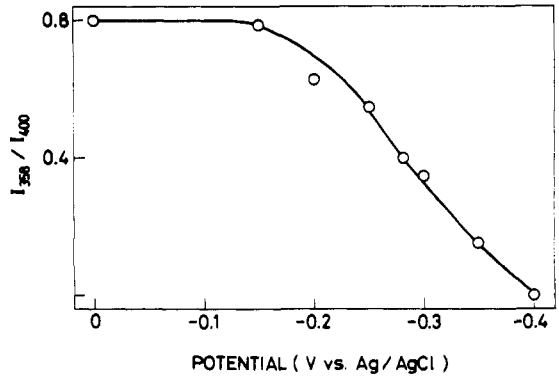

Figure 4. Electrode potential dependence of the intensity ratio, I_{358}/I_{400}, observed for the SERRS spectra of (TPP)$Cr^{III}Cl$ adsorbed on the silver electrode surface (see text).

chromium TPP complex so that the reduction does not cause any change in the structure.

Figure 4 summarizes the intensity ratio, I_{358}/I_{400}, of the SERRS spectra as a function of the electrode potential. The figure clearly illustrates a precipitous decrease of the ratio as the potential ranges between −0.15 and −0.35 V; actually, the surface spectrum at −0.4 V gives no feature at 358 cm^{-1}, only those at 401 and 337 cm^{-1}, the latter of which is observed as a shoulder in Figure 3E. In order to explain the spectral change observed for the trivalent complex on the electrode surface in the potential range from 0 to −0.4 V, we measured the potential dependence of the RRS and SERRS spectra of (TPP)$Cr^{III}ClO_4$, which is summarized in Figure 5. As

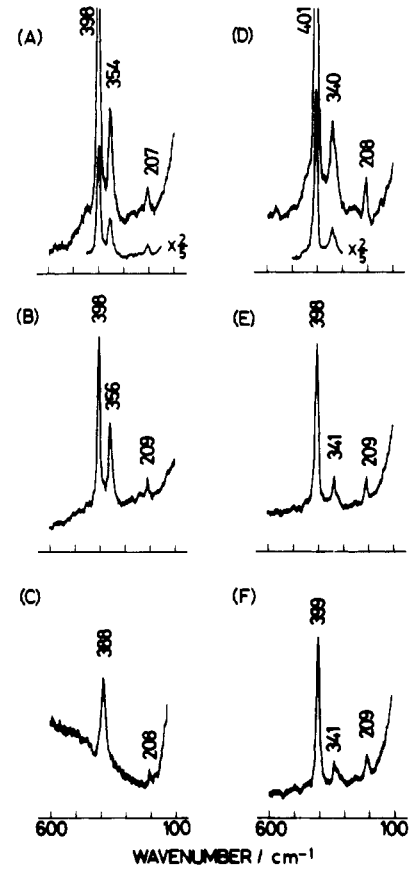

Figure 5. Electrode potential dependence of the RRS spectra (A–C) and the SERRS spectra (D–F) of (TPP)$Cr^{III}ClO_4$ in ACN (concentration of sample solution for RRS measurement 1.5×10^{-4} mol/L; concentration for SERRS measurement 6.3×10^{-5} mol/L): (A, D) at 0 V; (B, E) at −0.5 V; (C, F) at −1.0 V. Excitation wavelength = 457.9 nm. Laser power = 90 (A–C), 10 (D), 40 (E), 60 mW (F). Spectral slit width = 8 cm^{-1}.

already mentioned, the complex dissociates the perchlorate ion in ACN. The intensity ratio of the RRS band near 355 cm^{-1} to that at 398 cm^{-1} in Figure 5A,B is much smaller than the corresponding ratio of the RRS spectra of (TPP)$Cr^{III}Cl$ in Figure 3A,B. This proves that the small intensity ratio is characteristic of the dissociated complex, $[(TPP)Cr^{III}]^+$. On adsorption to the silver electrode surface, $[(TPP)Cr^{III}]^+$ shows the SERRS spectra illustrated in Figure 5D,E. The adsorbate does not show any change in spectral features in the potential range from 0 to −0.5 V, exhibiting SERRS bands near 400 and 340 cm^{-1}, which correspond to those at 401 and 337 cm^{-1} in Figure 3E. The spectral features in Figure 5D,E are almost identical to those of the SERRS spectrum observed for the adsorbate from (TPP)$Cr^{III}Cl$ at −0.4 V (not shown). Thus, upon adsorption to the electrode surface in ACN at −0.4 V, (TPP)$Cr^{III}Cl$ completely dissociates the chloride axial ligand. In addition, the similarity between the RRS spectrum of (TPP)$Cr^{III}Cl$ at 0 V (Figure 3A) and the SERRS spectrum of the complex at 0 V (Figure 3D) indicates that the electrode-adsorbed (TPP)$Cr^{III}Cl$ (at 0 V) retains the chloride ion as the fifth ligand. On the basis of these results, we can conclude that the drastic decrease in I_{358}/I_{400} observed for the SERRS spectra of (TPP)$Cr^{III}Cl$ is due to the conversion from the associated complex to the dissociated one. Assuming that the population ratio of (TPP)$Cr^{III}Cl$ to the total chromium complexes adsorbed at the electrode surface is 100% at 0 V and 0% at −0.4 V, we can interpret the curve in Figure 4 as indicating the change in the population ratio as a function of the electrode potential. When the potential was swept back to 0 from −0.4 V, the population ratio is recovered to the level of about 50%. Probably some of the released chloride ions are fixed at the electrode surface and coordinated again to the central metal ion, forming (TPP)$Cr^{III}Cl$ during the potential sweep back to 0 V. The remainder of the

released chloride ions, however, diffuse from the electrode surface during the potential sweep to −0.4 V; this is one of the main reasons for the partial recovery of the population ratio at 0 V.

As mentioned above, the 400- and 358-cm^{-1} bands are assigned to the ν_8 (A_{1g}) and γ_2 (A_{1u}) modes, respectively.[25,26] Presumably, the γ_2 mode of (TPP)$Cr^{III}Cl$ is enhanced because of the vibrational coupling between the out-of-plane mode and in-plane ring vibrations through a Cr–Cl stretching vibration. In the case of the manganese complexes, the intensity ratio of the γ_2 to ν_8 mode is insensitive to the dissociation of the axial ligand, as can be seen from the RRS spectra of the associated and dissociated manganese complexes (Figure 1A,C). The Cr(III) ion, with a relatively small ionic radius (0.62 Å), is expected to lie essentially in the averaged plane of the nitrogen atoms of the trivalent chromium complexes,[18] while the Mn(III) ion is largely out of the N_4 plane in the manganese complexes.[28] Also, the coupling of the γ_2 mode with the in-plane vibrations of the manganese complexes is expected to differ from that of the chromium complex; this may explain the insensitivity of the intensity ratio observed for the manganese complex.

The potential dependence of the adsorption state of (TPP)-$Cr^{III}Cl$ suggests that an electrostatic interaction is one of the main features contributing to the stabilization of the adsorbate on the electrode. That is, in the potential region between 0 and −0.15 V, where positive charges are abundant at the electrode surface, the associated chromium complex is stabilized to a larger extent than the dissociated complex through an electrostatic attraction between the chloride ion axial ligand and the positive surface charges. Upon a sweep of the electrode potential to the cathodic region, the amount of positive charges is reduced, stabilizing the dissociated complex relative to the associated one.

As mentioned above, (TPP)$Mn^{III}Cl$ dissociates the chloride ion on adsorption to the electrode at 0 V. The manganese complex has the high-spin d^4 configuration, while the chromium complex has the d^3 configuration, causing a stronger Cr–Cl bond than a Mn–Cl bond.[18] In addition, the displacement of the Mn(III) ion from the N_4 plane of the dissociated manganese complex may decrease an electrostatic repulsion between the positive surface charges and the central metal ion, rendering the dissociated complex state as a stable adsorbate at 0 V. In order to clarify the different adsorption behaviors of the manganese and chromium complexes, however, more detailed studies are required, including a study of the effect of the nature of axial ligands and solvents on the potential dependence of the SERRS spectra of the manganese and chromium complexes.

Relationship between Axial Ligation States and Electrochemical Properties of the Manganese and Chromium Complexes. In order to correlate the adsorption states and the electrochemical properties of the complexes, cyclic voltammograms of (TPP)$Mn^{III}X$ and (TPP)$Cr^{III}X$ (X = Cl^-, ClO_4^-) in ACN were recorded by using an anodized silver electrode. The results are summarized in Figure 6. The cyclic voltammograms observed for (TPP)$Mn^{III}Cl$ and (TPP)$Mn^{III}ClO_4$ (Figure 6A,B) indicate that the metal-centered reduction of these complexes on the silver electrode is reversible with almost identical half-wave potentials ($E_{1/2}$) of −0.19 V. The identity of the half-wave potentials can be explained by considering that during the electron-transfer process the adsorbates from the two manganese complexes assumes an identical structure at the electrode surface, as proved by the SERRS spectra. Although several authors[19,20] have already postulated a dissociation of the chloride axial ligand induced by an applied electrode potential before the metal-centered reduction of metalloporphines, the SERRS result in this paper is the first direct proof for the dissociation. The cyclic voltammograms for (TPP)$Cr^{III}Cl$ and (TPP)$Cr^{III}ClO_4$ (Figure 6C,D) show reduction peaks ($E_{p,c}$) at −0.39 and −0.79 V and at −0.92 V, respectively. The features are broad and exhibit no reoxidation peak, which is indicative of an irreversible (or slow) electron-transfer process. $E_{p,c}$ at −0.79 V for (TPP)$Cr^{III}Cl$ corresponds to that at −0.92 V for (TPP)-$Cr^{III}ClO_4$ and is ascribed to the metal-centered reduction process.

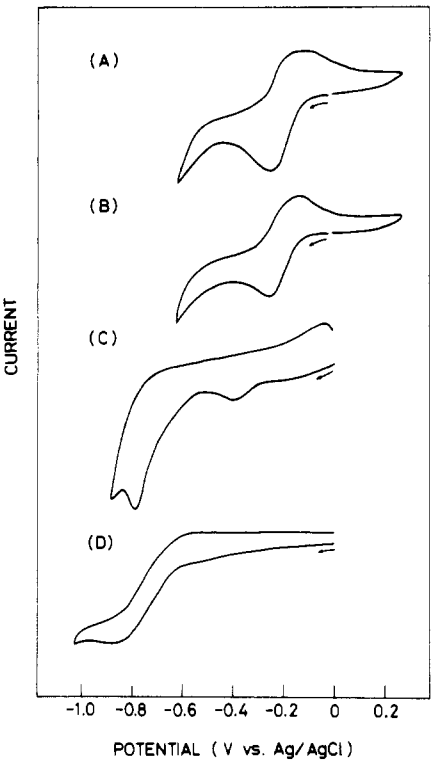

Figure 6. Cyclic voltammograms observed for (TPP)$Mn^{III}X$ and (TPP)$Cr^{III}X$ (X = Cl^-, ClO_4^-) by using an anodized silver electrode in ACN containing TBAP (8×10^{-2} mol/L; concentration of sample 3×10^{-4} mol/L; scan rate of electrode potential 500 mV/s): (A) (TPP)-$Mn^{III}Cl$; (B) (TPP)$Mn^{III}ClO_4$; (C) (TPP)Cr^{III}; (D) (TPP)$Cr^{III}ClO_4$.

$E_{p,c}$ at −0.39 V observed for the former complex is ascribable to the dissociation of the axial ligand from (TPP)$Cr^{III}Cl$; this is supported by the absence of the corresponding peak in the cyclic voltammograms of (TPP)$Cr^{III}ClO_4$ (Figure 6D). The irreversibility of the metal-centered reduction of the TPP chromium complexes in nonaqueous solvents has been extensively studied by using spectrophotometric and electrochemical methods.[19,20] The results indicated that the axial ligand environment about the central metal determines the nature of the metal-centered reduction of (TPP)$Cr^{III}X$ and that, when an axial ligand coordinates to the central metal as in the case of (TPP)$Cr^{III}Cl$ and (TPP)-$Cr^{III}ClO_4$ in dichloromethane, an irreversible reduction

$$(TPP)Cr^{III}X + e^- \rightarrow (TPP)Cr^{II} + X^-$$

takes place following the reaction, giving $E_{p,c}$ at −0.97 V (vs Ag/AgCl) for (TPP)$Cr^{III}Cl$ and at −0.77 V for (TPP)$Cr^{III}ClO_4$.[20] The difference in $E_{p,c}$ has been explained on the basis of stabilization of the central metal ion by the axially bound chloride ion, making the reduction process more difficult than in the case of (TPP)$Cr^{III}ClO_4$ (by 200 mV). As mentioned above, on adsorption to the silver electrode surface, both the chloride and perchlorate complexes in ACN dissociate the axial ligands prior to the reduction process and still show an appreciable difference in $E_{p,c}$ (−0.79 V for former complex and −0.92 V for the latter). The chloride ion has a strong affinity for the silver electrode surface, while the perchlorate ion shows no affinity for the surface.[29] There are two possible effects of the coadsorbed chloride ion on the chromium reduction process: (i) the chloride ion may cause the adsorbate to assume an orientation such that the reduction proceeds more easily than in the case of the perchlorate complex; (ii) the chloride ion may serve as a mediator in the electron transfer from the electrode to $[(TPP)Cr^{III}]^+$, making the reduction easier compared to that in the absence of the coadsorbed chloride ion. In order to clarify these points, however, a more direct and sensitive probe to monitor the reduction processes is required.

(28) Tulinsky, A.; Chen, B. M. *J. Am. Chem. Soc.* **1977**, *99*, 3646.

(29) Schmidt, E.; Stucki, S. *Ber. Bunsen-Ges. Phys. Chem.* **1973**, *77*, 913.